Int. J. Multiphase Flow Vol. 19, No. 3, pp. 501–507, 1993
Printed in Great Britain

0301-9322/93 $6.00 + 0.00
Pergamon Press Ltd

BUBBLE DISPERSION IN FREE SHEAR FLOWS

C. W. STEWART and C. T. CROWE
Department of Mechanical and Materials Engineering, Washington State University, Pullman, WA 99164-2920, U.S.A.

(Received 28 June 1992; in revised form 31 December 1992)

Abstract—The Stokes number defined in terms of the particle aerodynamic response time is not appropriate for bubble dispersion. Since the aerodynamic response time for bubbles is always very short, acceleration of the surrounding liquid always controls their motion. Thus, the ratio of local to gravitational acceleration is a better measure. The equation for relative bubble motion shows that an inverse Froude number, defined as the ratio of terminal bubble rise velocity to the characteristic velocity fluctuation, has the same interpretation for bubble dispersion as does the Stokes number for particles. This is demonstrated computationally for a sparse bubble swarm rising through a Stuart vortex.

Key Words: bubbles, dispersion, two-pulse phase flow, turbulence, free shear flow

1. INTRODUCTION

For gas–particle flows, Crowe *et al.* (1985) found that the Stokes number, St, defined as the ratio of the aerodynamic response time of the particle to the characteristic time of large-scale turbulence structures, is the controlling parameter for particle dispersion in a gas flow. Particles with $St \ll 1$ tend to remain in dynamic equilibrium with the fluid and are strongly dispersed by turbulence. If $St \gg 1$, the particles are not affected by the fluid motion and pass through with little or no dispersion.

The behavior of bubbles in a liquid is fundamentally different from that of solid particles in a gas. Bubbles have essentially no mass compared to the surrounding liquid, but particle inertia dominates the surrounding gas. Therefore, bubble motion leads the fluid while particles lag and the relative velocity is generally positive for bubbles but negative for particles. The aerodynamic response time measures how soon the bubble's relative velocity becomes limited by drag rather than how rapidly particles accelerate to match the surrounding flow.

Even after including the virtual mass to correct the response time, the St is not appropriate for bubble dispersion. The response time for even the largest bubbles is on the order of milliseconds. Since bubbles are always at the mercy of the fluid, a better measure of bubble dispersion should relate the relative strength of the accelerations that drive the bubble motion. We will show that the ratio of local acceleration to gravity is most appropriate.

2. BUBBLE DYNAMICS

To study the response of bubbles to the surrounding liquid, we require an expression for the relative velocity. We shall assume that the phase densities are constant, the bubbles are sufficiently sparse that there is no interaction, and there is no mass transfer between phases. Since we are concerned with motions of larger scale than the bubble size, we shall also neglect or average out smaller scale variations or turbulent fluctuations and surface tension effects. The local instantaneous momentum equation for phase k can be averaged by methods such as those used by Delhaye & Achard (1976), Nigmatulin (1979), Banerjee & Chan (1980), Kataoka & Serizawa (1989) and others to obtain, with the above assumptions,

$$\frac{\partial}{\partial t}\alpha_k \overline{\rho_k \mathbf{U}_k} + \nabla \cdot \alpha_k \overline{\rho_k \mathbf{U}_k \mathbf{U}_k} = \nabla \cdot \alpha_k \overline{\sigma_k} + \alpha_k \overline{\rho_k} \mathbf{g} + a \overline{\sigma_k \cdot \mathbf{n}_k}^{\mathrm{I}}. \quad [1]$$

Here σ_k is the stress tensor consisting of the usual pressure and shear components, $\alpha_k = V_k/V$ is the phase volume fraction, $\mathbf{g}$ is the gravity vector, $a = A_1/V$ is the interfacial area per unit volume

and $\mathbf{n}_k$ is the unit vector pointing out of phase k normal to the interface. The averages over a volume occupied by phase k and over the interfacial surface in that volume are indicated, respectively, by

$$\bar{X}_k \equiv \frac{1}{V_k}\int_{V_k} X_k \, \mathrm{d}V \quad \text{and} \quad \bar{X}_k^{\mathrm{I}} \equiv \frac{1}{A_{\mathrm{I}}}\int_{A_{\mathrm{I}}} X_k \, \mathrm{d}A.$$

Applying continuity to the momentum equation [1] and expanding the stress divergence, we obtain the following simplified expression for the acceleration of phase k:

$$\alpha_k \rho_k \frac{\mathrm{D}_k \mathbf{U}_k}{\mathrm{D}t} = \alpha_k \nabla \cdot \overline{\sigma_k} + \overline{\sigma_k} \cdot \nabla \alpha_k + \alpha_k \rho_k \mathbf{g} + a\,\overline{\sigma_k \cdot \mathbf{n}_k}^{\mathrm{I}}, \qquad [2]$$

where the material derivative following phase k is defined as

$$\frac{\mathrm{D}_k}{\mathrm{D}t} \equiv \frac{\partial}{\partial t} + \mathbf{U}_k \cdot \nabla.$$

The stress tensor is simplified by a decomposition similar to the method introduced by Banerjee & Chan (1980) for the pressure component. The total stress is split into a volume average, $\overline{\sigma_k}$, that varies on time and space scales larger than the dispersed phase, and a second that superimposes small variations of the same scales as the dispersed phase. The latter component consists of the average over the surface of each bubble or particle, $\Delta\bar{\sigma}_{k\mathrm{I}}$, and the variation around this average, $\Delta\sigma'_{k\mathrm{I}}$. This three-fold decomposition of the local instantaneous stress, σ_k, can be expressed as

$$\sigma_k \equiv \bar{\sigma}_k + \Delta\bar{\sigma}_{k\mathrm{I}} + \Delta\sigma'_{k\mathrm{I}}.$$

The interface average, $\Delta\bar{\sigma}_{k\mathrm{I}}$, is usually described as the pressure defect around a body moving through a fluid or the excess pressure on the surface of an expanding bubble (Stuhmiller 1977; Ruggles 1987). It can be taken as zero in the dispersed phase. Only the variation of the stress over the interfacial surface, $\Delta\sigma'_{k\mathrm{I}}$, can produce a net force on an individual bubble. But a gradient in the interface average stress, $\Delta\bar{\sigma}_{k\mathrm{I}}$, or in the dispersed phase volume fraction can generate a force in the continuous fluid. Applying this decomposition to the interfacial stress term in [2], noting that $\bar{\sigma}_k$ is constant with respect to the interface averaging operation, yields

$$a\,\overline{\sigma_k \cdot \mathbf{n}_k}^{\mathrm{I}} = \bar{\sigma}_k \cdot a\bar{\mathbf{n}}_k^{\mathrm{I}} + a\,\overline{\Delta\bar{\sigma}_{k\mathrm{I}} \cdot \mathbf{n}_k}^{\mathrm{I}} + a\,\overline{\Delta\sigma'_{k\mathrm{I}} \cdot \mathbf{n}_k}^{\mathrm{I}}. \qquad [3]$$

The first term on the RHS of [3] cancels with the second term on the RHS of [2] by virtue of the limiting form of the divergence theorem with Slattery (1972), Delhaye & Achard (1976), Nigmatulin (1979) and others have shown to give

$$\frac{1}{V}\int_{A_{\mathrm{I}}} \mathbf{n}_k \, \mathrm{d}A = -\nabla\alpha_k.$$

Application of the divergence theorem to the second term results in

$$a\,\overline{\Delta\bar{\sigma}_{k\mathrm{I}} \cdot \mathbf{n}_k}^{\mathrm{I}} = -\nabla\alpha_k \, \Delta\bar{\sigma}_{k\mathrm{I}}.$$

Prosperetti & Jones (1984) obtained the same result for pressure. But Banerjee & Chan (1980), Pauchon & Banerjee (1986) and others assume the interface average varies on the same scale as the volume average and is therefore essentially constant, moving the stress outside the divergence operator. However, regardless of which result is correct, we shall assume the bubble distribution is sufficiently dilute and uniform to neglect this term altogether.

The last term in [3] is the interfacial average of the surface-varying stress component. It represents the net force exerted on phase k by the interface. It can include life, the Basset force, viscous and form drag and the virtual mass effect. For bubbles, we can neglect all but the latter two forces. Using the subscripts c and d to indicate continuous and dispersed phases, respectively, the result is expressed as

$$a\,\overline{\Delta\sigma'_{\mathrm{dI}} \cdot \mathbf{n}_{\mathrm{d}}}^{\mathrm{I}} = -\alpha_{\mathrm{d}}\rho_{\mathrm{c}}K_{\mathrm{dc}}(\mathbf{U}_{\mathrm{d}} - \mathbf{U}_{\mathrm{c}}) - \alpha_{\mathrm{d}}\rho_{\mathrm{c}}C_{\mathrm{vm}}\left[\frac{\mathrm{D}_{\mathrm{d}}\mathbf{U}_{\mathrm{d}}}{\mathrm{D}t} - \frac{\mathrm{D}_{\mathrm{c}}\mathbf{U}_{\mathrm{c}}}{\mathrm{D}t}\right]. \qquad [4]$$

The first term in [4] is the standard inertial form of the interphase drag force. The second term represents the accepted form of the virtual mass force (Drew & Lahey 1987), where C_{vm} is the virtual mass coefficient. While the acceleration in [4] is not strictly objective (Pauchon & Smereka 1992), we shall consider the relative velocity gradients of sufficiently large scale compared to the bubbles that it is a good approximation in computing bubble trajectories.

Because we have neglected the effect of interface average stress and surface tension, and because the stress in the bubble is a uniform pressure to all practical intents, the liquid stress gradient effectively represents the external stress field for both phases. Substituting [4] into [2], including the simplifications to the interfacial stress terms, and recognizing that the interfacial force is symmetric, we obtain the following expressions for the acceleration for the dispersed and continuous phases, respectively:

$$\alpha_d \rho_d \frac{D_d \mathbf{U}_d}{Dt} + \alpha_d \rho_c C_{vm} \left[\frac{D_d \mathbf{U}_d}{Dt} - \frac{D_c \mathbf{U}_c}{Dt} \right] = \alpha_d \rho_d \mathbf{g} + \alpha_d \nabla \cdot \sigma_c - \alpha_d \rho_c K_{dc} (\mathbf{U}_d - \mathbf{U}_c) \quad [5]$$

and

$$\alpha_c \rho_c \frac{D_c \mathbf{U}_c}{Dt} - \alpha_d \rho_c C_{vm} \left[\frac{D_d \mathbf{U}_d}{Dt} - \frac{D_c \mathbf{U}_c}{Dt} \right] = \alpha_c \rho_c \mathbf{g} + \alpha_c \nabla \cdot \sigma_c - \alpha_d \rho_c K_{dc} (\mathbf{U}_d - \mathbf{U}_c) \quad [6]$$

We can eliminate the stress gradient between [5] and [6], and re-arrange the result into a single expression that gives the *relative velocity*, $\mathbf{U}_R = \mathbf{U}_d - \mathbf{U}_c$, in terms of liquid acceleration and gravity:

$$\frac{D_d \mathbf{U}_R}{Dt} + \mathbf{U}_R \cdot \nabla \mathbf{U}_c + \frac{\left(1 + \frac{\alpha_d}{\alpha_c}\right) K_{dc}}{\frac{\rho_d}{\rho_c} + \left(1 + \frac{\alpha_d}{\alpha_c}\right) C_{vm}} \mathbf{U}_R = \frac{1 - \frac{\rho_d}{\rho_c}}{\frac{\rho_d}{\rho_c} + \left(1 + \frac{\alpha_d}{\alpha_c}\right) C_{vm}} \left[\frac{D_c \mathbf{U}_c}{Dt} - \mathbf{g} \right], \quad [7]$$

where the total derivative of $\mathbf{U}_R$ follows the dispersed phase through the identity

$$\frac{D_d \mathbf{U}_d}{Dt} - \frac{D_c \mathbf{U}_c}{Dt} \equiv \frac{D_d \mathbf{U}_R}{Dt} + \mathbf{U}_R \cdot \nabla \mathbf{U}_c.$$

Since the RHS of [7] is identically zero for neutrally buoyant particles, there is no relative motion unless the phases have different densities or the motion is imposed as an initial condition. The sign of the right side depends on the density ratio so that heavy particles must move slower and light ones faster than the fluid. This is why bubbles always lead and solid particles always lag the fluid field. The same sign change on the gravity term makes particles fall and bubbles rise.

The third term on the LHS of [7] serves to limit the relative velocity—bubbles from moving too fast and particles from travelling too slow relative to the surrounding fluid. The inverse of the coefficient of $\mathbf{U}_R$ in this term is the aerodynamic response time for the system. We can simplify this by defining the phase drag coefficient, K_{dc}, in terms of the discrete drag coefficient, C_D, for a spherical body by

$$K_{dc} = \frac{3}{4} \frac{C_D}{D_d} |\mathbf{U}_d - \mathbf{U}_c|.$$

For nonspherical entities, the actual diameter can be replaced by the equivalent diameter, D_e, the diameter of a sphere of equal volume. Using this expression for K_{dc} and considering only a single particle ($\alpha_d \ll \alpha_c$), gives the expression

$$t_A = \frac{4}{3} \frac{\left(\frac{\rho_d}{\rho_c} + C_{vm}\right) D_d}{|\mathbf{U}_R| C_D}. \quad [8]$$

The denominator of [8] is a constant in Stokes flow or whenever the drag coefficient has inverse Re dependence. Substitution of the Stokes drag law, $C_D = 24/\mathrm{Re}$, gives the response time for very small, spherical bubbles as

$$t_A = C_{vm} \frac{\rho_c D_d^2}{18 \mu_c}.$$

For larger bubbles in the transition from spherical to ellipsoidal shape at higher Re Moore's (1962) analytically derived result, $C_D = 48/Re$, can be used in place of Stokes law. For still larger Taylor cap bubbles, where the gravitational acceleration dominates, one can substitute Davies & Taylor's (1950) formula for the terminal rise velocity to obtain

$$t_A = C_{vm}\sqrt{\frac{D_e}{2g}},$$

where D_e is the equivalent diameter. Ellipsoidal bubbles have a nearly constant terminal velocity except in very pure liquids (Clift *et al.* 1978). This implies that their response time is also approximately constant. Since the transition from ellipsoidal to Taylor cap occurs at an Eötvös number of 40 (Bhaga & Weber 1981), the response time can be estimated with the Taylor expression above using an equivalent diameter corresponding to Eö = 40, i.e.

$$D_e = \sqrt{\frac{40\sigma}{\rho_c g}}.$$

Using these expressions we find that a 0.5 mm diameter spherical bubble in water has a response time of about 3 ms. The response time of a typical ellipsoidal bubble of 1 cm equivalent diameter is about 15 ms and that of a larger Taylor cap bubble of 5 cm equivalent diameter is only about 25 ms. Thus, even a very large bubble has a very short response time. Bubble motion is always determined by external accelerations and the traditional St criterion developed by solid particles is not appropriate to describe bubble dispersion.

3. DISPERSION MODEL

In order to determine the proper measure of dispersion for bubbles, we need to investigate bubble behavior in the coherent flow structures of a free shear flow. To do this we shall model a plane mixing layer with Stuart's vortex, as Crowe *et al.* (1985) have done with particles. Stuart's vortex simulates the large-scale structures quite well, but does not model vortex pairing or spreading of the mixing layer. The two-dimensional vortex is defined by the two components of liquid velocity:

$$U_c(x, y, t) = U_0 t + \frac{\Delta U_0 \sinh(y)}{2[\cosh(y) + w\cos(x - U_0 t)]} \quad [9a]$$

and

$$V_c(x, y, t) = \frac{\Delta U_0 w \sinh(x - U_0 t)}{2[\cosh(y) + w\cos(x - U_0 t)]} \quad [9b]$$

where U_0 is the average x-velocity of the two layers and ΔU_0 is the difference in the speeds of the two streams. The parameter, w, determines the vortex rotation direction and aspect ratio. The structure is most realistic when $w = -0.25$.

We choose a reference frame that moves with the vortices so that $U_0 = 0$ and the high- and low-speed streams appear to flow in opposite directions at equal speeds. This makes ΔU_0 twice the speed of one of the opposing streams. We shall choose $\Delta U_0 = 2$ m/s. The shape of the flow field in this Stuart vortex is illustrated by the paths of neutral density particles in figure 1. Bubble velocities are compared with a simplified form of [7]. The bubble velocity is retained instead of converting to relative velocity and the bubble density and volume fraction are considered insignificant compared to those of the liquid. This converts [7] to

$$C_{vm}\frac{D_d \mathbf{U}_d}{Dt} = (1 + C_{vm})\frac{D_c \mathbf{U}_c}{Dt} - \mathbf{g} - K_{dc}(\mathbf{U}_d - \mathbf{U}_c). \quad [10]$$

Bubble trajectories are computed by solving the finite-difference analog of [10] for velocity, with the liquid velocity field given by [9], and integrating to obtain the time-dependent bubble position. Bubbles are initially released from zero relative velocity in a uniformly spaced 9×3 grid placed just below the horizontal axis of the vortex sheet outlined by the rectangle in figure 1. The divergence of bubble trajectories starting from different locations shows the dispersion. No bubble interaction is considered, in accordance with the original assumptions.

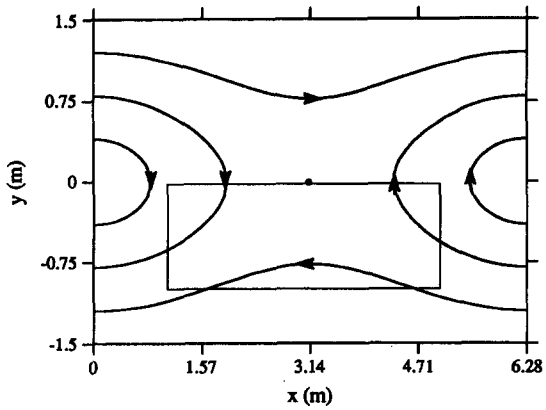

Figure 1. Stuart vortex configuration.

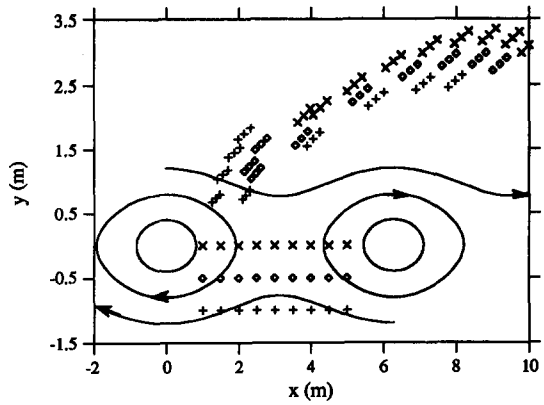

Figure 2. Taylor cap bubbles, $D_e = 50$ mm.

4. RESULTS AND DISCUSSION

Figures 2, 3 and 4 show the dispersion of grids of Taylor cap, ellipsoidal and spherical bubbles (equivalent diameters of 50, 5 and 0.5 mm, with terminal rise speeds of 50, 30 and 6 cm/s), respectively, 8–10 s after release in a Stuart vortex sheet with $\Delta U_0 = 2$. Three sequential bubble positions, 0.2 s apart, are plotted to indicate velocity as well as position. It is clear that the larger the bubble, the faster the rise speed and the smaller the dispersion. The larger bubbles in figure 2 maintain approximately their initial grid orientation, while the small spherical bubbles are well-mixed by the left-hand vortex. Recall that even the largest bubbles have a very short response time and tend to follow the motion of the liquid very closely. But, with gravity perpendicular to the vortex sheet, the bubble terminal rise speed relative to the liquid determines how strongly they are affected by the vortices.

Figure 5 shows the paths of each of the three bubble sizes after release in the lower right quadrant of a vortex, shown by the dotted streamines. The small, spherical bubble follows the vortex streamlines closely with very little rise evident. The ellipsoidal and cap bubbles, on the other hand, rise through the vortex with some change of course but clearly cross vortex streamlines. It is clear that bubbles exhibit an effect similar to that of the St for particles, but it is related to *residence time* instead of response time. That is, small bubbles that rise slowly spend more time in a turbulent eddy and conform more closely to its shape, while a large fast bubble passes right through. The ratio of residence times of the liquid to the bubble, the inverse ratio of their velocities, measures whether the bubble responds more to the acceleration of gravity or of the liquid. Define

$$Q \equiv \frac{\mathbf{U}_R}{\Delta \mathbf{U}_c}, \qquad [11]$$

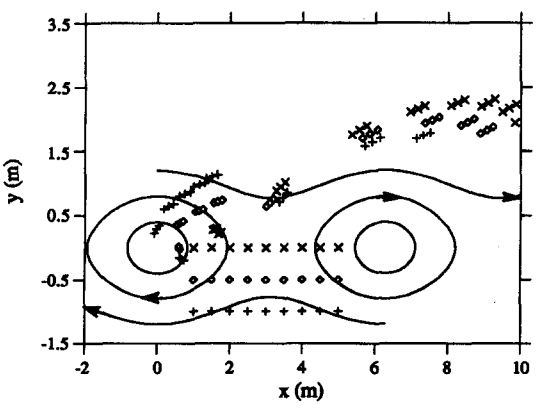

Figure 3. Ellipsoidal, $D_e = 5$ mm.

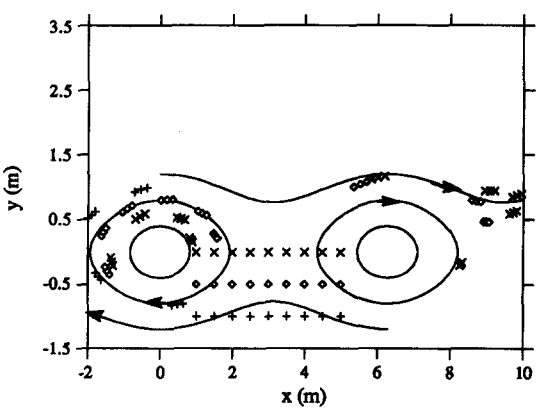

Figure 4. Spherical bubbles, $D_e = 0.5$ mm.

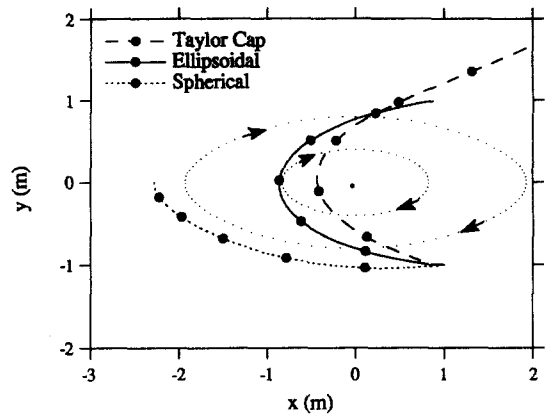

Figure 5. Single particle paths through a vortex.

where $\mathbf{U}_R$ is the bubble's terminal rise velocity and $\Delta\mathbf{U}_c$ is the characteristic velocity difference of the turbulent structure. For our Stuart vortex, the latter would be $\Delta\mathbf{U}_0 = 2$ m/s. Under this definition, a small value of Q indicates a slow rise speed and a strong response to fluctuations in the liquid. A relatively large Q means a strong response to gravity relative to the liquid motion and relatively little dispersion of the bubbles by liquid fluctuation.

The relation of gravity to liquid velocity fluctuation is made more clear by substituting Davies & Taylor's (1950) expression for terminal rise velocity for $\mathbf{U}_R$ in [11]. This makes our new quantity a ratio of gravity to inertia forces, which is equivalent to an inverse turbulent Froude number:

$$Q = \sqrt{\frac{\mathbf{g}D_e}{2\Delta\mathbf{U}_c^2}} = \frac{1}{\mathrm{Fr}}. \qquad [12]$$

For the viscous range, a similar substitution for the rise velocity using $C_D = 48/\mathrm{Re}$, yields

$$Q = \frac{1}{36}\frac{\rho_c \mathbf{g} D_e^2}{\Delta\mathbf{U}_c \mu_c} = \frac{1}{36}\left[\frac{\mathbf{g}D_e}{\Delta\mathbf{U}_c^2}\right]\left[\frac{\rho_c \Delta\mathbf{U}_c D_e}{\mu_c}\right] = \frac{1}{36}\frac{\mathrm{Re}}{\mathrm{Fr}^2}. \qquad [13]$$

The inverse Fr relation appears again, although to a power of 2. Substituting values representing the flows, we find that the large cap bubbles in figure 2 have $Q \approx 0.25$ via [12], while the small spherical ones in figure 4 have $Q \approx 0.03$ by [13]. The ellipsoidal bubbles in figure 3 have an intermediate $Q \approx 0.15$. Thus, the values of Q are consistent with the behavior illustrated in the figures.

5. CONCLUSION

Having compared the dispersion behavior of gas–liquid (bubble) flow to solid–gas (particulate) flow, we find that the St based on aerodynamic response time does not describe bubble dispersion, because the bubble response time is always extremely short regardless of bubble size. However, it appears from computational results that the ratio of gravitational to liquid acceleration does determine bubble dispersion characteristics. This same effect occurs with solid particles, but large particles that respond to gravity also have a very large aerodynamic response time so that the normal St criterion remains accurate.

A new quantity, defined as the ratio of terminal bubble rise velocity to the characteristic liquid velocity fluctuation, has the same interpretation for bubble dispersion as does the St for particles. The new quantity turns out to be equivalent to an inverse Fr, as might be expected intuitively.

Acknowledgements—This research was supported by the Northwest College and University Association for Science (Washington State University) under Grant DE-FG06-89ER-75522 with the U.S. Department of Energy.

REFERENCES

BANERJEE, S. & CHAN, A. M. C. 1980 Separated flow model, I. analysis of the averaged and local instantaneous formulation. *Int. J. Multiphase Flow* **6,** 1–24.

BHAGA, D. & WEBER, M. E. 1981 Bubbles in viscous liquids: shapes, wakes and velocities. *J. Fluid Mech.* **105,** 61–85.

CLIFT, R., GRACE, J. R. & WEBER, M. E. 1978 *Bubbles, Drops and Particles.* Academic Presss, New York.

CROWE, C. T., GORE, R. A. & TROUT, T. R. 1985 Particle dispersion by coherent structures in free shear flows. *Particulate Sci. Technol.* **3,** 149–158.

DAVIES, R. M. & TAYLOR, SIR G. 1950 The mechanics of large bubbles rising through extended liquids and through liquids in tubes. *Proc. R. Soc. Lond.* **A200,** 375–390.

DELHAYE, J. M. & ACHARD, J. L. 1976 On the averaging operations introduced in two-phase flow modelling. *Proc. 1st OECD/NEA Spec. Mtg on Transient Two-phase Flow*, Toronto, Vol. 1, pp. 5–84.

DREW, D. A. & LAHEY, R. T. 1987 The virtual mass and lift force on a sphere in rotating and straining inviscid flow. *Int. J. Multiphase Flow* **13,** 1–24.

KATAOKA, I. & SERIZAWA, A. 1989 Basic equations of turbulence in gas–liquid two-phase flow. *Int. J. Multiphase Flow* **15,** 113–121.

MOORE, D. W. 1962 The boundary layer on a spherical gas bubble. *J. Fluid Mech.* **16,** 161–176.

NIGMATULIN, R. I. 1979 Spatial averaging in mechanics of heterogeneous and dispersed systems. *Int. J. Multiphase Flow* **5,** 353–385.

PAUCHON, C. & BANERJEE, S. 1986 Interphase momentum interaction effects in the averaged multifield model. Part I: void propagation in bubbly flows. *Int. J. Multiphase Flow* **12,** 559–573.

PAUCHON, C. & SMEREKA, P. 1992 Momentum interactions in dispersed flow: an average and a variational approach. *Int. J. Multiphase Flow* **18,** 65–87.

PROSPERETTI, A. & JONES, A. V. 1984 Pressure forces in disperse two-phase flow. *Int. J. Multiphase Flow* **10,** 425–440.

RUGGLES, A. E. 1987 The propagation of pressure perturbations in bubbly air/water flows. Ph.D. Thesis, RPI, Troy, NY.

SLATTERY, J. C. 1972 *Momentum, Energy, and Mass Transfer in Continua.* Krieger, New York.

STUHMILLER, J. H. 1977 The influence of interfacial pressure forces on the character of two-phase flow model equations. *Int. J. Multiphase Flow* **3,** 551–560.